

# A rare-cell detector for cancer

Robert T. Krivacic\*, Andras Ladanyi<sup>†</sup>, Douglas N. Curry\*, H. B. Hsieh\*, Peter Kuhn<sup>‡</sup>, Danielle E. Bergsrud<sup>†</sup>, Jane F. Kepros<sup>†</sup>, Todd Barbera<sup>§</sup>, Michael Y. Ho\*, Lan Bo Chen<sup>¶</sup>, Richard A. Lerner<sup>‡</sup>, and Richard H. Bruce\*<sup>||</sup>

\*Scripps-PARC Institute for Advanced Biomedical Science, Palo Alto Research Center, 3333 Coyote Hill Road, Palo Alto, CA 94304; <sup>†</sup>Synta Pharmaceuticals Corporation, 45 Hartwell Avenue, Lexington, MA 02421; <sup>‡</sup>Scripps-PARC Institute for Advanced Biomedical Science, The Scripps Research Institute, 10550 North Torrey Pines Road, La Jolla, CA 92037; <sup>§</sup>Cima Potentica, Ltd, 74 Jersey Street, Marblehead, MA 01945; and <sup>¶</sup>Dana-Farber Cancer Institute, Harvard Medical School, 44 Binney Street, Boston, MA 02115

Contributed by Richard A. Lerner, June 7, 2004

Although a reliable method for detection of cancer cells in blood would be an important tool for diagnosis and monitoring of solid tumors in early stages, current technologies cannot reliably detect the extremely low concentrations of these rare cells. The preferred method of detection, automated digital microscopy (ADM), is too slow to scan the large substrate areas. Here we report an approach that uses fiber-optic array scanning technology (FAST), which applies laser-printing techniques to the rare-cell detection problem. With FAST cytometry, laser-printing optics are used to excite 300,000 cells per sec, and emission is collected in an extremely wide field of view, enabling a 500-fold speed-up over ADM with comparable sensitivity and superior specificity. The combination of FAST enrichment and ADM imaging has the performance required for reliable detection of early-stage cancer in blood.

Occult tumor cells (OTCs) shed from tumors can travel through the blood stream to anatomically distant sites and form metastatic disease, the major cause of cancer-related death in patients with solid tumors. These disseminated cells are present in circulation in extremely low concentrations, estimated to be in the range of one tumor cell in the background of  $10^6$ – $10^7$  normal blood cells and are occult to routine imaging and laboratory studies (1). Automated digital microscopy (ADM) using image analysis for recognition of specifically labeled tumor cells has been demonstrated to be the most reliable method currently available for OTC detection (2–5).

However, at the typical scan rate of 800 cells per sec, ADM is too slow to screen for a statistically valid number of OTCs (6). This slow scan rate is a result of two factors. One is the substantial latency associated with stepping the sample under the microscopy objective. This stepping results from the lens' small field of view. The other factor is the long exposure time that is due to the low level of excitation from broadband illumination sources and the lack of sensitivity of the charge-coupled device detector used for imaging.

Here we report a scanning instrument using fiber-optic array scanning technology (FAST) that can locate OTCs at a rate that is 500 times faster than ADM, with comparable sensitivity and improved specificity. The exposure time is reduced by using a laser source for higher illumination levels and a more sensitive photomultiplier detector. However, our key innovation is providing an optical system with an exceptionally large field of view (50 mm) without a loss of collection efficiency. By collecting the fluorescence in an array of optical fibers that forms a wide collection aperture, the FAST cytometer has a 100-fold increase in field of view over ADM. Although this increase in field of view comes with a reduction in instrument resolution, the resolution is still sufficient for the identification of fluorescently labeled cells. This field of view is large enough to eliminate the need to step the sample under the collection optics, and hence there is no stepping latency. Although other instruments have used brighter sources and photomultiplier detectors (7), the FAST cytometer combines them with a large field of view and achieves a speed-up sufficient for efficient OTC detection in blood.

## Materials and Methods

**Cell Culture and Treatment.** HT29 cells were grown in McCoy's 5a medium containing 1.5 mM L-glutamine and 10% FBS. For modeling the *in vivo* situation of decreased epithelial cell adhesion molecule (Ep-CAM) expression of OTCs, HT29 cells were cultured for 3 days in the presence of 30 ng/ml IL-4 (BD Pharmingen) as described by Fleiger *et al.* (8). IL-4 treatment resulted in a 35% decrease of Ep-CAM expression as determined by direct immunofluorescence staining with anti-Ep-CAM fluorochrome-conjugated antibodies (Miltenyi Biotec, Bergisch Gladbach, Germany).

**Immunofluorescent Labeling.** Blood samples were processed by using a previously described method (9). Briefly, heparinized blood from human volunteers was spiked with HT29 colorectal cancer cells and subjected to lysis with isotonic ammonium chloride buffer (155 mM  $\text{NH}_4\text{Cl}$ /10 mM  $\text{KHCO}_3$ /0.1 mM EDTA, pH 7.4) at room temperature for 5 min. After centrifugation, the remaining white cell pellet was washed and resuspended in PBS, and the total number of living peripheral blood mononuclear cells was counted by using trypan blue exclusion. The cells were attached to custom-designed adhesive slides (Marienfeld, Bad Mergentheim, Germany) at 37°C for 60 min, and the slides then were blocked with cell culture medium at 37°C for 20 min. The deposited cells were fixed in ice-cold methanol for 5 min, rinsed in PBS, and blocked with 20% human AB serum (Nabi Diagnostics, Boca Raton, FL) in PBS at 37°C for 20 min. Slides then were incubated at 37°C for 1 h with a monoclonal anti-pan cytokeratin antibody (Sigma), which recognizes human cytokeratins 1, 4, 5, 6, 8, 10, 13, 18, and 19 in immunoblotting. Subsequently, slides were washed in PBS and incubated with a mixture of Alexa Fluor 488 and R-phycoerythrin-conjugated goat anti-mouse antibody (Molecular Probes) at 37°C for 30 min. After counterstaining with 0.5  $\mu\text{g}/\text{ml}$  4',6-diamidino-2-phenylindole (Molecular Probes) in PBS at room temperature for 10 min, slides were mounted in ProLong mounting medium (Molecular Probes).

**ADM.** Coordinates of prospective cells identified by the FAST cytometer were fed into the rare-event imaging system (REIS), a fully automated scanning digital microscopy system. The hardware components of the REIS and the proprietary scanning software have been described in detail elsewhere (4, 10).

**Immunomagnetic Enrichment.** IL-4-treated and nontreated HT29 cells were spiked into two separate aliquots of 2 ml of peripheral blood. After red blood cell lysis, samples were divided into two parts: the first part was deposited onto adhesive slides as described above. Before cell deposition, the second part was

Abbreviations: OTC, occult tumor cell; ADM, automated digital microscopy; FAST, fiber-optic array scanning technology; Ep-CAM, epithelial cell adhesion molecule; REIS, rare-event imaging system.

<sup>||</sup>To whom correspondence should be addressed. E-mail: richard.bruce@parc.com.

© 2004 by The National Academy of Sciences of the USA

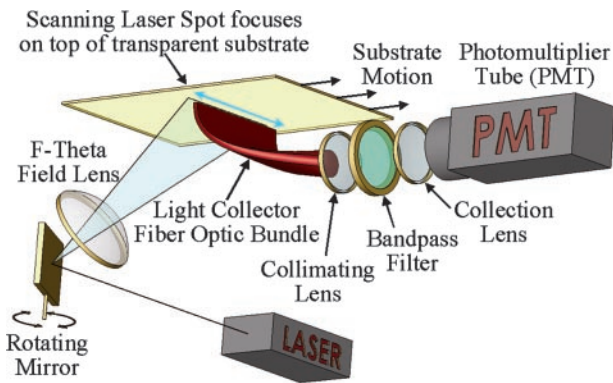


Fig. 1. Schematic of the optical path. [Reproduced with permission from ref. 27 (Copyright 2004, IEEE).]

subjected to positive immunomagnetic selection with anti-Ep-CAM microbeads (Miltenyi Biotec). The immunomagnetic enrichment was performed with MS separation columns (Miltenyi Biotec) according to manufacturer instructions.

## Results

**Optical System.** The large field of view is enabled by an optical fiber bundle with asymmetric ends. As shown in Fig. 1, the collection end is long (50 mm) and narrow (2 mm), whereas the transmission end is circular (11.3 mm in diameter). In operation, an argon ion laser scans the substrate lying on top of the collection end, and the collected emission is subsequently collimated after the circular aperture. The emission from the fluorescent probes is filtered by using standard dichroic filters before detection in a photomultiplier. The sample moves across the laser scan path on a stage traveling in a direction orthogonal to the laser scan direction. The location of a fluorescing cell is determined accurately by the scan and stage positions at the time of emission. The scanning mechanics enable accurate determination of the emission location (better than 100  $\mu\text{m}$ ) for subsequent reviewing.

The laser is scanned at 100 scans per sec by using a galvanometer-rotated mirror, whereas the substrate is moved at 2  $\text{mm}\cdot\text{sec}^{-1}$  over it, which produces an exposure rate of 1  $\text{cm}^2\cdot\text{sec}^{-1}$ . The galvanometer can operate at this scan velocity over a 25° scan angle with linear angular time response. An F-Theta field lens transforms the 15.2° actual mirror deflection into linear displacement with a transformation accuracy better than 0.1%, which results in a reproducible distortion over the field of <82  $\mu\text{m}$  that can be eliminated in the software. The 10- $\mu\text{m}$ -diameter focused beam is transformed into an elliptical spot size, 10  $\times$  20  $\mu\text{m}$ , by the 60° angle of incidence. The ellipse major axis, which is normal to the sweep direction, defines the

pixel resolution along one dimension. The sweep rate of 10  $\text{m}\cdot\text{sec}^{-1}$  defines the 1- $\mu\text{sec}$  transit time per pixel.

The intrinsic detection threshold of the FAST cytometer is currently determined by the autofluorescence from the borosilicate in the fiber optics and collimation lenses that is stimulated by scattered laser light. For 50 mW of laser power incident on a quartz substrate, this autofluorescence is  $\approx 15$  times the combination of all the other noise sources (such as noise in the electronics) and corresponds to the equivalent emission from  $\approx 1,000$  fluorescein molecules. For OTC detection, however, the measured autofluorescence from blood exceeds this intrinsic autofluorescence by 10-fold, and consequently, it is the autofluorescence from the blood that determines the effective detection threshold for this application.

A comparison of detection threshold between FAST and digital microscopy in the presence of blood autofluorescence was made by using a calibration slide containing a dilution series of Alexa Fluor 488 dye in rows differing in concentration by a factor of 2. Both instruments scanned the slides, and the signal strength for each row was compared with the strength of the autofluorescence coming from a blood sample under identical scanning conditions. In the presence of background autofluorescence, FAST can detect cell fluorescence that is approximately eight times dimmer than can be detected with a digital microscope. We attribute this difference to a combination of more efficient excitation of the Alexa Fluor 488 probe by the 488-nm laser and more efficient excitation of the blood autofluorescence by the microscope broadband mercury light source. This detection advantage enables FAST to detect cells with lower levels of fluorescence and, hence, lower levels of expressed target protein.

**Measurements.** Detected fluorescent objects are analyzed with software filter operations to differentiate rare cells from false positives. Because the cells are generally smaller than the laser-spot resolution (20  $\mu\text{m}$ ), the first filter passes all objects that are below a size threshold (20  $\mu\text{m}$ ). A second filter analyzes the ratio between the intensities of the fluorescence from different channels to eliminate homogeneous dye aggregates, a common artifact of immunofluorescence staining.

The FAST capability was tested with samples of HT29 cells spiked in peripheral blood from a healthy donor. The samples were scanned first by the REIS (10), an ADM with image-analysis software optimized for the detection of OTCs. The REIS scan along with visual inspection established the number of tumor cells. The samples then were scanned by the FAST cytometer.

Objects detected by the FAST cytometer were subsequently reexamined under a fluorescence microscope to differentiate rare cells from artifacts for annotation of the FAST image data. The false positives are distinguished from true positives by shape, staining pattern, and the presence of 4',6-diamidino-2-phenylindole-stained nuclear material. By visual inspection of the microscope images, we determined that the FAST

Table 1. Data for ADM and FAST cytometer scans of peripheral blood spiked with the HT29 cell line

Sample	Sample size, no. of WBCs	REIS OTCs, no. of cells	FAST OTCs, no. of cells	FAST false negatives, no. of cells	FAST sensitivity, %	FAST false positives, no. of objects	FAST specificity
1	6 $\times$ 10 <sup>6</sup>	76	69	7	91	79	1.3 $\times$ 10 <sup>-5</sup>
2	3 $\times$ 10 <sup>6</sup>	102	102	0	100	18	6 $\times$ 10 <sup>-6</sup>
3	4.5 $\times$ 10 <sup>6</sup>	200	198	2	99	106	2.4 $\times$ 10 <sup>-5</sup>
Total	13.5 $\times$ 10 <sup>6</sup>	378	369	9	98	203	1.5 $\times$ 10 <sup>-5</sup>

The sample is scanned first with REIS to determine the total number of OTCs and then scanned with the FAST cytometer. The false negatives are the cells missed by the FAST, and the sensitivity is the ratio of the OTCs detected by the FAST cytometer to the total OTCs. The false positives are artifacts detected by the FAST cytometer that are indistinguishable from OTCs. The specificity is the ratio of false positives detected by the FAST cytometer to the total number of white blood cells (WBCs) in the sample.

**Table 2. Scan data for ADM plus the tandem FAST cytometer and REIS for HT29-spiked peripheral blood**

Sample	Sample size, no. of WBCs	REIS OTCs, no. of cells	Tandem OTCs, no. of cells	Tandem false negatives, no. of cells	Tandem sensitivity, %	Tandem false positives, no. of objects	Tandem specificity
1	$6 \times 10^6$	76	65	11	86	13	$2 \times 10^{-6}$
2	$3 \times 10^6$	102	101	1	99	5	$1.7 \times 10^{-6}$
3	$4.5 \times 10^6$	200	196	4	98	19	$4 \times 10^{-6}$
Total	$13.5 \times 10^6$	378	362	16	95	37	$3 \times 10^{-6}$

The sample is scanned first with the REIS to determine the total number of OTCs. The sample is then scanned with the FAST cytometer, which identifies the locations of possible OTCs, and then REIS scans only these locations. The tandem OTCs are those found in this operation. The false negatives are the cells missed by the tandem operation, and the sensitivity is the ratio of the OTCs detected by the tandem operation to total OTCs. The false positives are artifacts detected by the FAST cytometer that are indistinguishable from OTCs. The specificity is the ratio of false positives detected by the tandem operation to the total number of white blood cells (WBCs) in the sample.

detection results in an average specificity of  $1.5 \times 10^{-5}$  and an average sensitivity of 98%, as shown in Table 1, while scanning at a rate of 300,000 cells per sec.

Although its scan rate is adequate to efficiently address the sample size needed in rare-cell detection, the FAST cytometer does not have the optical resolution needed for visual verification of true positive cells; consequently, the value of FAST scanning is in “enriching” the sample to reduce the amount of ADM imaging to a practical level. We investigated the FAST/ADM tandem approach with samples of cell-line-spiked blood. After the FAST scan, all of the FAST-identified objects were scanned again individually by the REIS using location information from the FAST scan. With a combination of FAST enrichment and REIS scanning, a sensitivity of 95% and specificity of  $3 \times 10^{-6}$  was achieved (as shown in Table 2).

An alternative approach for enrichment of OTCs is immunomagnetic technology, which has been used by many investigators in recent years to increase the sampling volume to accommodate for the low scan rate of digital microscopy (11). This enrichment technology utilizes magnetizable microbeads coated with an antibody to epithelial antigens to separate OTCs from normal hematopoietic cells. This technique has demonstrated a 50–80% recovery and 10- to 25-fold enrichment factor in cell culture models; however, its applicability *in vivo* has not been fully validated yet (12, 13). At issue is the dependence of cell recovery on the expression level of the target antigen. Because expression of several antigens that are targeted by the immunobeads were found to be frequently down-regulated in OTCs, the approach may have serious reliability problems in clinical samples. Examples of such down-regulated target antigens include Ep-CAM, the mucin-like glycoprotein, and the HER2/neu receptor (14–16).

To investigate the effect of expression level of the target antigen on cell recovery, HT29 colorectal cancer cells were cultured in the presence or absence of IL-4, a cytokine known to suppress Ep-CAM expression (8). Treated and nontreated cells were spiked into separate aliquots of blood samples from healthy donors. After ammonium chloride lysis of red blood cells, the spiked samples were divided into two parts and either subjected or not subjected to immunomagnetic enrichment before deposition onto adhesive slides. The enriched sample (containing  $\approx 20,000$  total cells) was scanned with REIS, and the nonenriched sample (containing  $\approx 6$  million total cells) was scanned with the FAST cytometer and REIS.

As shown in Fig. 2, although FAST cytometry and REIS are equally sensitive in detecting untreated cells, immunomagnetic enrichment causes a 50% cell loss. Furthermore, whereas the 35% decrease in expressed target antigen had no effect on the detection level of FAST cytometry and REIS, immunomagnetic enrichment causes a 2.5 times reduction in OTC recovery.

## Discussion

It is estimated that OTCs are present in circulation at concentrations between  $10^{-6}$  and  $10^{-7}$  (1). Assuming the lower end of this range,  $10^{-7}$ , a sample of at least 100 million hematopoietic cells is needed to detect at least one OTC with a high probability (99.995%). An ADM analysis of such a sample size would take 18 h, resulting in 3,000–30,000 objects for a cytopathology examination (2–5). Based on the performance presented here, a FAST prescan of 100 million cells would take 5 min and result in 1,500 objects for subsequent rescanning by ADM. With the improved specificity of the tandem approach, this rescanning with ADM would require subsequent manual examination of only 300 objects. With the tandem approach, the task of screening 100 million hematopoietic cells could be completed within 1 h.

Unlike enrichment approaches, no additional processing is required for FAST cytometry that could result in reduced sensitivity due to cell loss. In addition, unlike alternative techniques for OTC detection such as PCR or fluorescence-activated cell sorting, FAST cytometry allows the cytomorphology of the prospective rare cells to be readily examined at any time.

The availability of a scanning system with the speed and sensitivity of FAST could have a profound impact on the management of cancer patients. First, because tumor cells are estimated to be dispersed into the circulation at the earliest stages of malignant progression, it could be used for the early

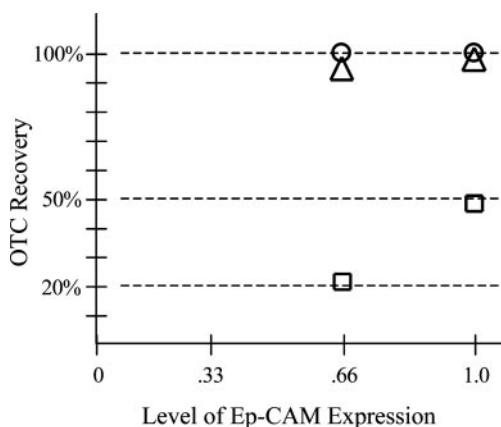


**Fig. 2.** Cell recovery comparison. Cell recovery of HT29 cells in peripheral blood is compared with and without immunomagnetic enrichment. The cell recovery with enrichment ( $\square$ ) is measured with REIS, and the cell recovery without enrichment is measured by both REIS ( $\circ$ ) and FAST cytometry ( $\triangle$ ). The measurements are made for two levels of expression of Ep-CAM, the target antigen for immunomagnetic enrichment.

diagnosis of cancer (17, 18). Although, there are some data suggesting that the concentration of OTCs in the blood increases with advanced-stage disease, the literature for early-stage detection is contradictory because of the absence of reliable methodology for the detection of rare cells at these low concentrations (19–22). The investigation of large sample sizes accessible through FAST cytometry should enable a more valid study of OTC concentration as a function of disease progression.

Second, because OTC numbers have been shown to correlate with therapy response, FAST cytometry could be a valuable tool for the identification of patients at high risk for relapse, enabling the initiation of more aggressive therapy tailored to individual patient needs (23, 24). Finally, the high throughput of FAST cytometry could enable screening of high-risk populations as a general test for the detection of cancer cells. Subsequent tests using tissue-specific markers could be used for the characterization of the tissue of origin. In addition, FAST could be used as a research tool to locate and pool OTCs in sufficient quantities for subsequent cytological/molecular studies (25, 26).

To improve FAST specificity further to reduce the number of objects that need to be rescanned by the ADM and hence the rescan time, modifications may be made to the optical path to enable dual laser excitation. With this modification, a second laser with 532-nm excitation could be used to excite the red fluorophore much more efficiently than the 488-nm excitation currently being used, which would enable a substantial reduction

in the dye concentration and would be expected to reduce aggregation. With higher resolution, more accurate shape information could be used in the image-analysis process to reject false-positive detections.

Although validation of the technology on samples from early- and late-stage cancer patients is still incomplete, preliminary results show that FAST image-analysis filters are adequate for detecting OTCs in cancer patient peripheral blood, although these OTCs are not nearly as uniform in shape as are tumor cell lines. Because the resolution of its scan is much lower than that of ADM, FAST is insensitive to morphological variation, and consequently, the sensitivity and specificity of the FAST assay is more independent of OTC heterogeneity than an ADM assay, which relies on morphological analysis for filtering.

OTCs constitute the link between primary and metastatic lesions, and after the removal of known primary or metastatic lesions, they constitute the actual target of therapy. Consequently, a better understanding of these cells will provide critical information about the metastatic potential, drug sensitivity, and development of therapy resistance in metastasizing tumors. The simplicity of the FAST approach provides a technology base for a low-cost, robust, clinical diagnostic instrument that could be used for the early diagnosis of cancer and for monitoring the efficacy of anticancer therapy for solid tumors. FAST cytometry could become as essential and ubiquitous as the Pap smear for cancer diagnosis.

1. Pantel, K. & Otte, M. (2001) *Semin. Cancer Biol.* **11**, 327–237.
2. Borgen, E., Naume, B., Nesland, J. M., Nowels, K. W., Pavlak, N., Ravkin, I. & Goldbard, S. (2001) *Cytometry* **46**, 215–221.
3. Bauer, K. D., de la Torre-Bueno, J., Diel, I. J., Hawes, D., Deckerm, W. J., Priddy, C., Bossy, B., Ludmann, S., Yamamoto, K., Masih, A. S., *et al.* (2000) *Clin. Cancer Res.* **6**, 3552–2559.
4. Kraeft, S. K., Sutherland, R., Gravelin, L., Hu, G. H., Ferland, L. H., Richardson, P., Elias, A. & Chen, L. B. (2000) *Clin. Cancer Res.* **6**, 434–442.
5. Mehes, G., Lorch, T. & Ambros, P. F. (2000) *Cytometry* **42**, 357–362.
6. Bajaj, S., Welsh, J. B., Leif, R. C. & Price, J. H. (2000) *Cytometry* **39**, 285–294.
7. Pachmann, K., Heiss, P., Demel, U. & Titz, G. (2001) *Clin. Chem. Lab. Med.* **39**, 811–817.
8. Flieger, D., Hoff, A. S., Sauerbruch, T. & Schmidt-Wolf, I. G. (2001) *Clin. Exp. Immunol.* **123**, 9–14.
9. Kraeft, S. K., Salgia, R. & Chen, L. B. (2003) *Methods Mol. Med.* **75**, 423–430.
10. Kraeft, S. K., Ladanyi, A., Galiger, K., Herlitz, A., Sher, A. C., Bergsrud, D. E., Even, G., Brunelle, S., Harris, L., Salgia, R., *et al.* (2004) *Clin. Cancer Res.* **10**, 3020–3028.
11. Witzig, T. E., Bossy, B., Kimlinger, T., Roche, P. C., Ingle, J. N., Grant, C., Donohue, J., Suman, V. J., Harrington, D., Torre-Bueno, J., *et al.* (2002) *Clin. Cancer Res.* **8**, 1085–1091.
12. Naume, B., Borgen, E., Nesland, J. M., Beiske, K., Gilen, E., Renolen, A., Ravnas, G., Qvist, H., Karesen, R. & Kvalheim, G. (1998) *Int. J. Cancer* **78**, 556–560.
13. Martin, V. M., Siewert, C., Scharl, A., Harms, T., Heinze, R., Ohl, S., Radbruch, A., Miltenyi, S. & Schmitz, J. (1998) *Exp. Hematol.* **26**, 252–264.
14. Thurm, H., Ebel, S., Kentenich, C., Hensen, A., Riethdorf, S., Coith, C., Wallwiener, D., Braun, S., Oberhoff, C., Janicke, F., *et al.* (2003) *Clin. Cancer Res.* **9**, 2598–2604.
15. Braun, S., Hepp, F., Sommer, H. L. & Pantel, K. (1999) *Int. J. Cancer* **84**, 1–5.
16. Kasimir-Bauer, S., Otterbach, F., Oberhoff, C., Schmid, K. W., Kimmig, R. & Seeber, S. (2003) *Int. J. Mol. Med.* **12**, 969–975.
17. Butler, T. P. & Gullino, P. M. (1975) *Cancer Res.* **35**, 512–516.
18. Schmidt-Kittler, O., Ragg, T., Daskalakis, A., Granzow, M., Ahr, A., Blankenstein, T. J., Kaufmann, M., Diebold, J., Arnholdt, H., Muller, P., *et al.* (2003) *Proc. Natl. Acad. Sci. USA* **100**, 7737–7742.
19. Nakamura, T., Yasumura, T., Hayashi, K., Eguchi, R., Ide, H., Takasaki, K. & Kasajima, T. (2000) *Anticancer Res.* **20**, 4739–4744.
20. Kim, S. J., Ikeda, N., Shiba, E., Takamura, Y. & Noguchi, S. (2001) *Breast Cancer* **8**, 63–69.
21. Wong, I. H., Yeo, W., Chan, A. T. & Johnson, P. J. (2001) *Cancer Lett.* **162**, 65–73.
22. Weihrauch, M. R., Skibowski, E., Koslowsky, T. C., Voiss, W., Re, D., Kuhn-Regnier, F., Bannwarth, C., Siedek, M., Diehl, V. & Bohlen, H. (2002) *J. Clin. Oncol.* **20**, 4338–4343.
23. Racila, E., Euhus, D., Weiss, A. J., Rao, C., McConnell, J., Terstappen, L. W. & Uhr, J. W. (1998) *Proc. Natl. Acad. Sci. USA* **95**, 4589–4594.
24. Terstappen, L. W., Rao, C., Gross, S. & Weiss, A. J. (2000) *Int. J. Oncol.* **17**, 573–578.
25. Klein, C. A., Seidl, S., Petat-Dutter, K., Offner, S., Geigl, J. B., Schmidt-Kittler, O., Wendler, N., Passlick, B., Huber, R. M., Schlimok, G., *et al.* (2002) *Nat. Biotechnol.* **20**, 387–392.
26. Kraus, J., Pantel, K., Pinkel, D., Albertson, D. G. & Speicher, M. R. (2003) *Genes Chromosomes Cancer* **36**, 159–166.
27. Curry, D. N., Krivacic, R. T., Hsieh, H. B., Ladanyi, A., Bergsrud, D. E., Ho, M. Y., Chen, L. B., Kuhn, P. & Bruce, R. H. (2004) *Proceedings of IEEE Engineering in Medicine and Biology Society (IEEE, Piscataway, NJ)*, Vol. 26.